J|A|C|S ARTICLES

Published on Web 07/06/2009

Solid-State and Solution NMR Studies of the CAP-Gly Domain of Mammalian Dynactin and Its Interaction with Microtubules

Shangjin Sun,[†] Amanda Siglin,[‡] John C. Williams,*[,‡] and Tatyana Polenova*[,†]

Department of Chemistry and Biochemistry, University of Delaware, Newark, Delaware 19716, and Department of Molecular Medicine, Beckman Research Institute of City of Hope, 1500 East Duarte Road, Duarte, California 91010

Received March 14, 2009; E-mail: JWilliams@coh.org; tpolenov@mail.chem.udel.edu

Abstract: Microtubules (MTs) and microtubule binding proteins (MTBPs) play fundamental physiological roles including vesicle and organelle transport, cell motility, and cell division. Despite the importance of the MT/MTBP assemblies, there remains virtually no structural or dynamic information about their interaction at the atomic level due to the inherent insolubility and lack of long-range order of MTs. In this study, we present a combined magic angle spinning solid-state and solution NMR study of the MTBP CAP-Gly domain of mammalian dynactin and its interaction with paclitaxel-stabilized microtubules. We report resonance assignments and secondary structure analysis of the free CAP-Gly in solution and in the solid state by a combination of two- and three-dimensional homo- and heteronuclear correlation spectra. In solution, binding of CAP-Gly to microtubules is accompanied by the broadening of the majority of the peaks in HSQC spectra except for the residues at the termini, precluding further structural analysis of the CAP-Gly/microtubule complexes. In the solid state, DARR spectra of free CAP-Gly and its complex with microtubules display well-resolved lines, permitting residue-specific resonance assignments. Interestingly, a number of chemical shifts in the solid-state DARR spectra of the CAP-Gly/microtubule complex are perturbed compared to those of the free CAP-Gly, suggesting that conformational changes occur in the protein upon binding to the microtubules. These results indicate that CAP-Gly/microtubule assemblies are amenable to detailed structural characterization by magic angle spinning NMR spectroscopy and that solid-state NMR is a viable technique to study MT/protein interactions in general.

Introduction

Microtubules represent one of the three essential types of cytoskeletal elements in cells. Together with their associated proteins, microtubules play important roles in a broad range of physiological functions, encompassing cell migration, mitosis, polarization and differentiation, and vesicle and organelle transport.[1] Microtubule-associated proteins have been implicated in numerous diseases, ranging from motor neuron and degenerative disorders to neoplasia and viral infections.[2−11]

Dynactin multisubunit assembly is the activator of the cytoplasmic microtubule-based dynein retrograde motor complex.[12] Dynactin binds the dynein motor complex and is responsible for the long-range dynein movement along microtubules (MTs). The principal component of the dynactin complex is the p150^{Glued} subunit (reviewed in ref 12). This subunit contains a microtubule-binding domain (MTBD) and two predicted coiled coil regions; the first is reported to bind to dynein, and the second contains the binding site for the Arp1 rod proteins. The precise mechanism that enables dynactin to participate in many functions remains unclear; however, its ability to bind to MTs through the CAP-Gly domain appears to be critical for many of these processes.

CAP-Gly motifs were originally identified as glycine-rich (Gly) domains in four cytoskeleton-associated proteins (CAPs).[13,14] CAP-Gly domains are conserved in organisms from yeast to humans; they are responsible for microtubule binding in vitro.[15,16] Recent efforts have demonstrated that CAP-Gly domains play central roles in many proteins, including the p150^{Glued} subunit of dynactin,[12] cytoplasmic

[†] University of Delaware.
[‡] Beckman Research Institute of City of Hope.

(1) Vale, R. D. *Cell* **2003**, *112*, 467–480.
(2) Chevalier-Larsen, E.; Holzbaur, E. L. F. *Biochim. Biophys. Acta* **2006**, *1762*, 1094–1108.
(3) Duncan, J. E.; Goldstein, L. S. B. *PLoS Genet.* **2006**, *2*, 1275–1284.
(4) Fung, L. F.; Lo, A. K. F.; Yuen, P. W.; Liu, Y.; Wang, X. H.; Tsao, S. W. *Life Sci.* **2000**, *67*, 923–936.
(5) Gerdes, J. M.; Katsanis, N. *Cell. Mol. Life Sci.* **2005**, *62*, 1556–1570.
(6) Guo, Y.; Petrof, B. J.; Hussain, S. N. A. *Muscle Nerve* **2001**, *24*, 1468–1475.
(7) National Institutes of Health NINDS Web site. http://www.ninds.nih.gov/disorders/motor_neuron_diseases/detail_motor_neuron_diseases.htm.
(8) Stokin, G. B.; Goldstein, L. S. B. *Annu. Rev. Biochem.* **2006**, *75*, 607–627.
(9) Stokin, G. B.; Goldstein, L. S. B. *J. Physiol. (Paris)* **2006**, *99*, 193–200.
(10) Tan, G.; Lightcap, C. M.; Williams, J. C.; Schnell, M. J. *J. Neurovirol.* **2006**, *12*, 80–80.
(11) Vadlamudi, R. K.; Bagheri-Yarmand, R.; Yang, Z.; Balasenthil, S.; Nguyen, D.; Sahin, A. A.; den Hollander, P.; Kumar, R. *Cancer Cell* **2004**, *5*, 575–585.
(12) Schroer, T. A. *Annu. Rev. Cell. Dev. Biol.* **2004**, *20*, 759–79.
(13) Galjart, N. *Nat. Rev. Mol. Cell Biol.* **2005**, *6*, 487–498.
(14) Riehemann, K.; Sorg, C. *Trends Biochem. Sci.* **1993**, *18*, 82–83.
(15) Pierre, P.; Scheel, J.; Rickard, J. E.; Kreis, T. E. *Cell* **1992**, *70*, 887–900.
(16) Feierbach, B.; Nogales, E.; Downing, K. H.; Stearns, T. *J. Cell Biol.* **1999**, *144*, 113–124.

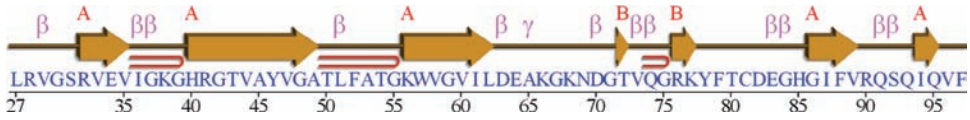

Figure 1. Amino acid sequence and secondary structure of the CAP-Gly domain of dynactin generated by PDBsum[84] from the X-ray coordinates deposited in the PDB file 3E2U.[26]

linker proteins (CLIPs and CLIPRs) such as CLIP170[17] and CLIPR59,[18] an α-tubulin folding factor,[16] tubulin chaperone,[19] the familial cylindormatosis cellular suppressor CYLD,[20] and the kinesin protein KIF13b.[21] It has been shown that mutations in the genes encoding the CAP-Gly domains lead to various disorders. For example, a missense point mutation, G59S, in the p150^{Glued} subunit of dynactin was identified in a family with lower motor neuron disease.[22,23] *In vivo* studies indicate that the binding affinity of the mutant to microtubules was reduced, and homology modeling suggests that this mutation destabilizes and leads to misfolding of the CAP-Gly motif.[22,24] Five other mutations, G71R, G71E, G71A, T72P, and Q74P, have been recently identified in patients with Perry syndrome, an autosomal dominant neurodegenerative disorder manifested in parkinsonism and weight loss and often accompanied by depression, social withdrawal, and suicidal attempts.[25] While the exact mechanism leading to pathogenicity of these mutants is unknown, they exhibit decreased microtubule binding (G71R and Q74P) and show redistribution of dynactin in transfected cells compared to the wild-type CAP-Gly.[25]

Further understanding of the mechanism of dynactin binding to the microtubule and its regulation of dynein-based cargo transport in the healthy (wild-type) and disease (G59S, G71R, G71E, G71A, T72P, and Q74P mutants) states requires the knowledge of the atomic-resolution structure of the CAP-Gly domains assembled on the microtubule. Several high-resolution structures of CAP-Gly domains of human dynactin and its complexes with EB1 and CLIP-170 have been reported recently,[26−29] and an additional structure has been deposited in the Protein Data Bank (accession number 2COY). In Figure 1, the amino acid sequence and secondary structures are shown for a CAP-Gly domain from human dynactin spanning residues 27−97 (PDB file 3E2U).[26] The binding interfaces of CAP-Gly with these proteins have been determined from the X-ray structures and using chemical shift perturbations.[26–29] On the basis of the crystal structure of the CAP-Gly domain from *Caenorhabditis elegans* F53F4.3 protein, it has been hypothesized that the highly conserved GKNDG motif would interact with microtubules.[19] However, the large molecular weight/insolubility and lack of long-range order of CAP-Gly/microtubule assemblies have to date prevented their high-resolution structural and dynamics studies by X-ray crystallography or solution NMR spectroscopy, and the interface between the CAP-Gly and polymerized microtubules remains unresolved, particularly at atomic resolution. Alternative high-resolution structural methodologies are therefore needed that do not require soluble or crystalline preparations. Magic angle spinning (MAS) NMR methods present such a technique and are becoming increasingly important for structural studies of uniformly and extensively enriched microcrystalline and membrane proteins,[30−56]

(17) Scheel, J.; Pierre, P.; Rickard, J. E.; Diamantopoulos, G. S.; Valetti, C.; van der Goot, F. G.; Haner, M.; Aebi, U.; Kreis, T. E. *J. Biol. Chem.* **1999**, *274*, 25883–25891.
(18) Perez, F.; Pernet-Gallay, K.; Nizak, C.; Goodson, H. V.; Kreis, T. E.; Goud, B. *J. Cell Biol.* **2002**, *156*, 631–642.
(19) Li, S. L.; et al. *J. Biol. Chem.* **2002**, *277*, 48596–48601.
(20) Saito, K.; et al. *Structure* **2004**, *12*, 1719–1728.
(21) Venkateswarlu, K.; Hanada, T.; Chishti, A. H. *J. Cell Sci.* **2005**, *118*, 2471–2484.
(22) Puls, I.; Jonnakuty, C.; LaMonte, B. H.; Holzbaur, E. L. F.; Tokito, M.; Mann, E.; Floeter, M. K.; Bidus, K.; Drayna, D.; Oh, S. J.; Brown, R. H.; Ludlow, C. L.; Fischbeck, K. H. *Nat. Genet.* **2003**, *33*, 455–456.
(23) Mojsilovic-Petrovic, J.; Jeong, G. B.; Crocker, A.; Arneja, A.; David, S.; Russell, D.; Kalb, R. G. *J. Neurosci.* **2006**, *26*, 9250–9263.
(24) Levy, J. R.; Sumner, C. J.; Caviston, J. P.; Tokito, M. K.; Ranganathan, S.; Ligon, L. A.; Wallace, K. E.; LaMonte, B. H.; Harmison, G. G.; Puls, L.; Fischbeck, K. H.; Holzbaur, E. L. F. *J. Cell Biol.* **2006**, *172*, 733–745.
(25) Farrer, M. J.; et al. *Nat. Genet.* **2009**, *41*, 163–165.
(26) Weisbrich, A.; Honnappa, S.; Jaussi, R.; Okhrimenko, O.; Frey, D.; Jelesarov, I.; Akhmanova, A.; Steinmetz, M. O. *Nat. Struct. Mol. Biol.* **2007**, *14*, 959–967.
(27) Hayashi, I.; Plevin, M. J.; Ikura, M. *Nat. Struct. Mol. Biol.* **2007**, *14*, 980–1.
(28) Hayashi, I.; Wilde, A.; Mal, T. K.; Ikura, M. *Mol. Cell* **2005**, *19*, 449–60.
(29) Honnappa, S.; Okhrimenko, O.; Jaussi, R.; Jawhari, H.; Jelesarov, I.; Winkler, F. K.; Steinmetz, M. O. *Mol. Cell* **2006**, *23*, 663–71.
(30) McDermott, A.; Polenova, T.; Bockmann, A.; Zilm, K. W.; Paulsen, E. K.; Martin, R. W.; Montelione, G. T. *J. Biomol. NMR* **2000**, *16*, 209–219.
(31) Marulanda, D.; Tasayco, M. L.; McDermott, A.; Cataldi, M.; Arriaran, V.; Polenova, T. *J. Am. Chem. Soc.* **2004**, *126*, 16608–16620.
(32) Marulanda, D.; Tasayco, M. L.; Cataldi, M.; Arriaran, V.; Polenova, T. *J. Phys. Chem. B* **2005**, *109*, 18135–18145.
(33) Yang, J.; Paramasivan, S.; Marulanda, D.; Cataidi, M.; Tasayco, M. L.; Polenova, T. *Magn. Reson. Chem.* **2007**, *45*, S73–S83.
(34) Yang, J.; Tasayco, M. L.; Polenova, T. *J. Am. Chem. Soc.* **2008**, *130*, 5798–5807.
(35) Pauli, J.; Baldus, M.; van Rossum, B.; de Groot, H.; Oschkinat, H. *ChemBioChem* **2001**, *2*, 272–281.
(36) Castellani, F.; van Rossum, B.; Diehl, A.; Schubert, M.; Rehbein, K.; Oschkinat, H. *Nature* **2002**, *420*, 98–102.
(37) Bockmann, A.; Lange, A.; Galinier, A.; Luca, S.; Giraud, N.; Juy, M.; Heise, H.; Montserret, R.; Penin, F.; Baldus, M. *J. Biomol. NMR* **2003**, *27*, 323–339.
(38) Ernst, M.; Detken, A.; Bockmann, A.; Meier, B. H. *J. Am. Chem. Soc.* **2003**, *125*, 15807–15810.
(39) Paulson, E. K.; Morcombe, C. R.; Gaponenko, V.; Dancheck, B.; Byrd, R. A.; Zilm, K. W. *J. Am. Chem. Soc.* **2003**, *125*, 15831–15836.
(40) Igumenova, T. I.; McDermott, A. E.; Zilm, K. W.; Martin, R. W.; Paulson, E. K.; Wand, A. J. *J. Am. Chem. Soc.* **2004**, *126*, 6720–6727.
(41) Jaroniec, C. P.; MacPhee, C. E.; Bajaj, V. S.; McMahon, M. T.; Dobson, C. M.; Griffin, R. G. *Proc. Natl. Acad. Sci. U.S.A.* **2004**, *101*, 711–716.
(42) Zech, S. G.; Wand, A. J.; McDermott, A. E. *J. Am. Chem. Soc.* **2005**, *127*, 8618–8626.
(43) Heise, H.; Hoyer, W.; Becker, S.; Andronesi, O. C.; Riedel, D.; Baldus, M. *Proc. Natl. Acad. Sci. U.S.A.* **2005**, *102*, 15871–15876.
(44) Siemer, A. B.; Ritter, C.; Ernst, M.; Riek, R.; Meier, B. H. *Angew. Chem., Int. Ed.* **2005**, *44*, 2441–2444.
(45) Franks, W. T.; Zhou, D. H.; Wylie, B. J.; Money, B. G.; Graesser, D. T.; Frericks, H. L.; Sahota, G.; Rienstra, C. M. *J. Am. Chem. Soc.* **2005**, *127*, 12291–12305.
(46) Cady, S. D.; Hong, M. *Proc. Natl. Acad. Sci. U.S.A.* **2008**, *105*, 1483–1488.
(47) Li, Y.; Berthold, D. A.; Gennis, R. B.; Rienstra, C. M. *Protein Sci.* **2008**, *17*, 199–204.
(48) Bockmann, A. *C. R. Chim.* **2006**, *9*, 381–392.
(49) Frericks, H. L.; Zhou, D. H.; Yap, L. L.; Gennis, R. B.; Rienstra, C. M. *J. Biomol. NMR* **2006**, *36*, 55–71.
(50) De Paepe, G.; Bayro, M. J.; Lewandowski, J.; Griffin, R. G. *J. Am. Chem. Soc.* **2006**, *128*, 1776–1777.
(51) Hong, M. *Structure* **2006**, *14*, 1731–1740.

macromolecular assemblies,[47,57−61] and disordered fibrils.[62−66] Despite the recent rapid progress in the field, the number of proteins for which site-specific resonance assignments by MAS NMR have been accomplished remains small.

In this paper, we present a combined solid-state and solution NMR study of the CAP-Gly domain free and in complex with microtubules. We report site-specific resonance assignments and secondary structure analysis of CAP-Gly in solution and in the solid state by a combination of two- and three-dimensional NMR experiments. In solution, binding of CAP-Gly to polymerized microtubules is accompanied by the broadening of the majority of the peaks in the HSQC spectra except for the residues at the termini. At the same time, binding of CAP-Gly to nonpolymerized tubulin or to tubulin oligomers results in small but distinct chemical shift perturbations in several residues. The solid-state MAS NMR spectra of the CAP-Gly bound to the microtubules are well resolved, and chemical shift perturbations were observed for a number of residues, suggesting conformational changes upon formation of the complex. Our results indicate that magic angle spinning NMR methods can be used for high-resolution structural analysis of CAP-Gly/microtubule assemblies.

Results

Resonance Assignments and Torsion Angle Analysis of CAP-Gly in Solution. ^{15}N HSQC and a combination of HNCA, CBCA(CO)NH, HNCO, HN(CA)CO, and HBHA(CO)NH triple-resonance experiments were used to obtain essentially complete resonance assignments of backbone atoms as well as C_β and H_β (illustrated in Figure S1 and Table S1 of the Supporting Information). We employed TALOS[67] to analyze the ψ and ϕ torsion angles on the basis of the backbone assignments and the C_β shifts; the results are illustrated in Figure S1. The results indicate that a large portion of the residues are in the β-sheet conformation, which is consistent with the three-dimensional structures of other p150^{Glued} CAP-Gly domains (PDB files 2HQH,[27] 2HKN,[29] 2HKQ,[29] 3E2U,[26] and 1TXQ[28]).

Comparison of torsion angles predicted by TALOS with the experimental torsion angles in the five published X-ray structures above (illustrated in Figure S2 in the Supporting Information) reveals that for the majority of the residues the angles agree to within ±20°, with the exception of the following residues: G37-K38-G39, G48, G55, L62, K66, K68, D70, F79, G84-H85-G86. All of these residues are located in flexible loops or at the termini of the individual β-sheets; therefore, the discrepancy is not surprising. Overall, our results indicate that the secondary structure of CAP-Gly is generally consistent with the previous X-ray results.

Chemical shift assignments were also obtained from HSQC and HNCA spectra for a CAP-Gly sample prepared in phosphate buffer 7.0 (summarized in Table S2 of the Supporting Information). As illustrated in Figure S3 of the Supporting Information, the ^{1}H and the ^{15}N the chemical shifts for the majority of the residues are intact with notable exceptions of the ^{63}DEAKG^{67} and ^{84}GHGI^{87} regions of the protein belonging to flexible loops, which exhibited small chemical shift perturbations. Similarly, the $^{13}C^\alpha$ chemical shifts are only weakly pH-dependent (Figure S3) with the differences not exceeding 0.15 ppm for most of the residues, with the exception of A65 (0.2 ppm), V73 (0.3 ppm), G84 (−0.22 ppm), H85 (0.44 ppm), and G86 (−0.25 ppm).

Resonance Assignments and Torsion Angle Analysis of CAP-Gly by Magic Angle Spinning Solid-State NMR Spectroscopy. For resonance assignments of free CAP-Gly in the solid state, a combination of two- and three-dimensional homo- and heteronuclear correlation MAS NMR spectra were acquired at 14.1 and 21.1 T (Figures 2 and 3, Figures S4 and S5 of the Supporting Information). The 14.1 T DARR spectra were collected at several temperatures ranging from −1.7 to −34.9 °C to determine the best experimental conditions. The two-dimensional DARR spectra collected at 21.1 T and −15 °C show excellent resolution, and the ^{13}C line widths of 0.3−0.6 ppm indicate homogeneous sample preparation and are consistent with our previous observations for thioredoxin prepared by controlled precipitation from PEG.[31−33] Interestingly, at 14.1 T we observed severe line broadening with lowering of the temperature to −34.9 °C (illustrated in Figure S4 for the 14.1 T spectra); the narrow lines are restored upon increasing the temperature to −1.7 °C, indicating that the sample does not undergo irreversible deterioration. The broad lines at low temperatures may be due either to capturing multiple conformational states or to intermediate time scale motions under these conditions. This temperature dependence of DARR spectra is consistent with previous reports.[33,45] Additional relaxation measurements are necessary to understand the temperature dependence of the DARR spectra; these will be the subject of a future study. An observation of critical importance to the analysis of the spectra of the CAP-Gly/microtubule complex (vide infra) is that lowering of the temperature is accompanied by broadening of the lines for the majority of the cross-peaks with a finite number of peaks showing small but noticeable ^{13}C chemical shift changes on the order of 0.1 ppm and not exceeding 0.2 ppm (e.g., Thr C^α−C^β cross-peaks, as shown in the Supporting Information).

The ^{13}C chemical shifts are also field-independent, with the 14.1 and 21.1 T DARR spectra being virtually superimposable. While the majority of the one-bond correlations are present in both spectra, there are some notable differences: several cross-peaks corresponding to the Ile side chain correlations are present

(52) Kobayashi, M.; Matsuki, Y.; Yumen, I.; Fujiwara, T.; Akutsu, H. *J. Biomol. NMR* **2006**, *36*, 279–293.
(53) Lange, A.; Giller, K.; Hornig, S.; Martin-Eauclaire, M. F.; Pongs, O.; Becker, S.; Baldus, M. *Nature* **2006**, *440*, 959–962.
(54) Chen, L. L.; Kaiser, J. M.; Lai, J. F.; Polenova, T.; Yang, J.; Rienstra, C. M.; Mueller, L. J. *Magn. Reson. Chem.* **2007**, *45*, S84–S92.
(55) Chen, L.; Kaiser, J. M.; Polenova, T.; Yang, J.; Rienstra, C. M.; Mueller, L. J. *J. Am. Chem. Soc.* **2007**, *129*, 10650–10651.
(56) Varga, K.; Tian, L.; McDermott, A. E. *Biochim. Biophys. Acta—Proteins Proteomics* **2007**, *1774*, 1604–1613.
(57) Lorieau, J. L.; Day, L. A.; McDermott, A. E. *Proc. Natl. Acad. Sci. U.S.A.* **2008**, *105*, 10366–10371.
(58) Goldbourt, A.; Gross, B. J.; Day, L. A.; McDermott, A. E. *J. Am. Chem. Soc.* **2007**, *129*, 2338–2344.
(59) Baldus, M. *Curr. Opin. Struct. Biol.* **2006**, *16*, 618–623.
(60) Egawa, A.; Fujiwara, T.; Mizoguchi, T.; Kakitani, Y.; Koyama, Y.; Akutsu, H. *Proc. Natl. Acad. Sci. U.S.A.* **2007**, *104*, 790–795.
(61) Paik, Y.; Yang, C.; Metaferia, B.; Tang, S. B.; Bane, S.; Ravindra, R.; Shanker, N.; Alcaraz, A. A.; Johnson, S. A.; Schaefer, J.; O'Connor, R. D.; Cegelski, L.; Snyder, J. P.; Kingston, D. G. I. *J. Am. Chem. Soc.* **2007**, *129*, 361–370.
(62) Wickner, R. B.; Dyda, F.; Tycko, R. *Proc. Natl. Acad. Sci. U.S.A.* **2008**, *105*, 2403–2408.
(63) Wasmer, C.; Lange, A.; Van Melckebeke, H.; Siemer, A. B.; Riek, R.; Meier, B. H. *Science* **2008**, *319*, 1523–1526.
(64) Helmus, J. J.; Surewicz, K.; Nadaud, P. S.; Surewicz, W. K.; Jaroniec, C. P. *Proc. Natl. Acad. Sci. U.S.A.* **2008**, *105*, 6284–6289.
(65) van der Wel, P. C. A.; Lewandowski, J. R.; Griffin, R. G. *J. Am. Chem. Soc.* **2007**, *129*, 5117–5130.
(66) Chimon, S.; Shaibat, M. A.; Jones, C. R.; Calero, D. C.; Aizezi, B.; Ishii, Y. *Nat. Struct. Mol. Biol.* **2007**, *14*, 1157–1164.
(67) Cornilescu, G.; Delaglio, F.; Bax, A. *J. Biomol. NMR* **1999**, *13*, 289–302.

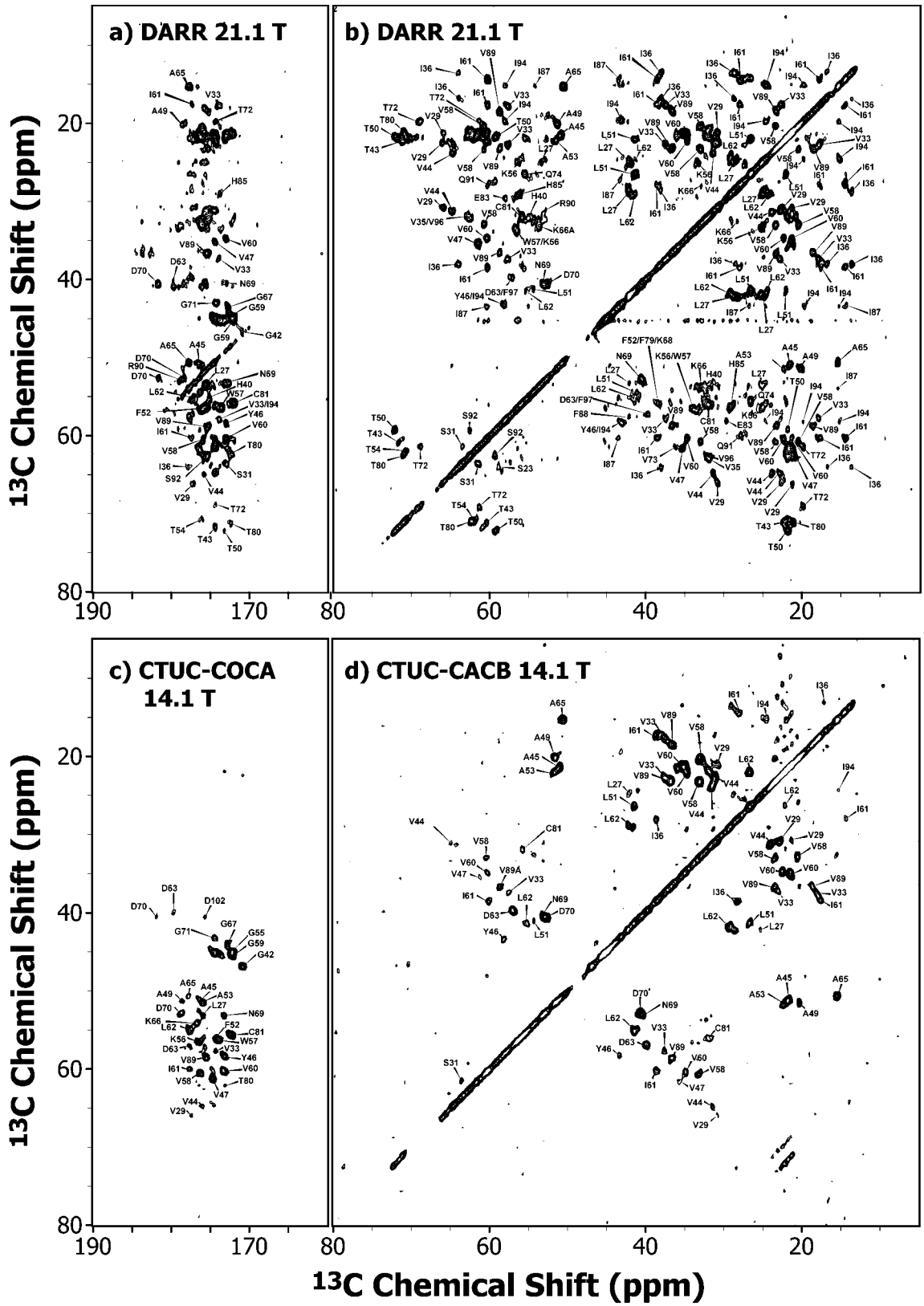

Figure 2. Two-dimensional solid-state MAS NMR spectra of CAP-Gly: carbonyl and aliphatic regions of the 21.1 T DARR spectrum (mixing time 50 ms) (a, b, respectively), scalar-based CTUC−COCA spectrum (c), scalar-based CTUC−CACB spectrum. Note that the resolution of the 14.1 T scalar-based spectra is similar to that of the 21.1 dipolar-based DARR data, in contrast to the lower resolution of the 14.1 T dipolar-based DARR spectrum (see the Supporting Information). The scalar-based experiments yield only single-bond correlations, while in the dipolar-based DARR data set a number of two- and three-bond cross-peaks are present. For DARR spectra, the first contour is set at 5σ, with a multiplier of 1.2.

only in the 21.1 T spectra, while side chain correlations corresponding to Pro residues appear only in the 14.1 T data set (shown in the Supporting Information). Therefore, both spectra were used in the analysis.

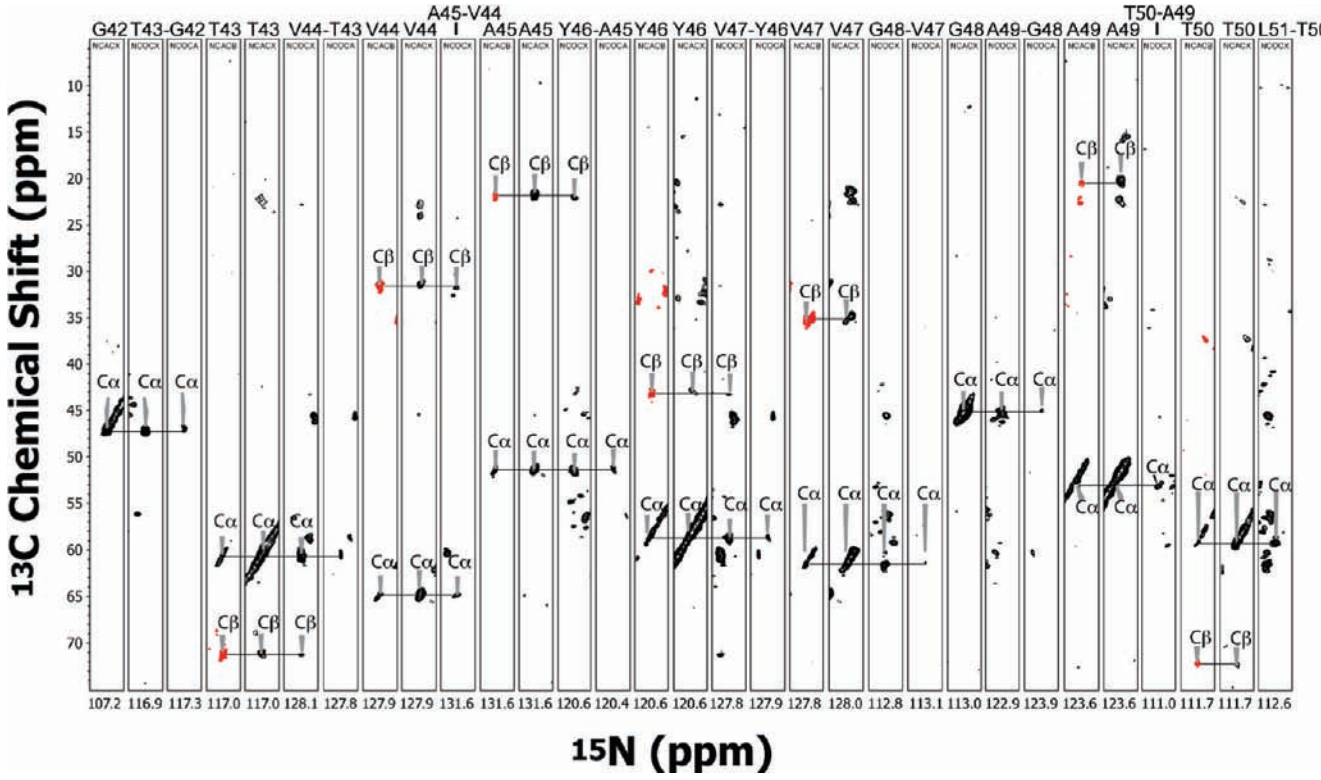

Figure 3. Backbone walk for G42−L51 using three-dimensional MAS experiments: dipolar-based NCOCX, NCACX, and NCACB and scalar-based NCOCA. Negative cross-peaks resulting from the two-bond N−C^{β} correlations in the NCACB spectra are shown in red. The contours are set as follows: NCACB, at 5σ; NCACX, at 4σ; NCOCX, at 5.5σ; NCOCA, at 4.5σ; with a multiplier of 1.2.

Comparison of the dipolar- and scalar-based spectra additionally reveals that, as expected, the resolution of the scalar-based 14.1 T CTUC−COCA and CTUC−CACB data sets (Figure 2 c,d) is superior compared to that of the 14.1 T dipolar DARR spectrum (Figure S5 of the Supporting Information) and is similar to that of the 21.1 T DARR spectrum. At the same time, due to the experimental limitations imposed by moderate MAS frequencies and moderate decoupling powers, we observed that magnetization transfer was generally not as efficient as in the DARR experiments, and a number of cross-peaks were weak or missing, notably three of seven Ala cross-peaks, all Thr $C^{\alpha}-C^{\beta}$ cross-peaks, and all Ser correlations with the exception of the S31 $C^{\alpha}-C^{\beta}$ cross-peak. Nevertheless, since scalar-based experiments yield solely one-bond correlations while the DARR spectrum acquired with a mixing time of 50 ms contains a number of two-bond cross-peaks, the simultaneous use of the scalar- and dipolar-based experiments proved beneficial for confirming assignments for a number of residues.

From the three-dimensional dipolar-based NCACB, NCACX, and NCOCX and the scalar-based NCOCA experiments, we have obtained nearly complete site-specific resonance assignments for CAP-Gly (chemical shifts tabulated in the Supporting Information). Figure 3 displays a backbone walk for G42−L51 using multiple data sets to illustrate the assignments. The majority of the peaks are present in the spectra, with the exception of those for the terminal residues S19, T20, E21, and E107. Additionally, the resonances corresponding to two proline residues, P26 and P106, could not be found in the 2D and 3D heteronuclear correlation data sets. While we have identified in the homonuclear 2D and 3D 14.1 T DARR spectra the side chain $C^{\beta}-C^{\gamma}$ and $C^{\gamma}-C^{\delta}$ cross-peaks that can be unequivocally attributed to prolines due to their appearance in the distinct region of the spectra, which does not contain cross-peaks from other types of residues (Figure 2), these proline cross-peaks could not be assigned site-specifically. A number of arginine, glutamate, and lysine residues appeared in crowded regions of the NCACB and NCACX spectra, but could be unequivocally identified from the correlations to their preceding or succeeding residues in the NCOCX and/or NCOCA data sets. L27 could not be unambiguously assigned because of the absence of sequential correlations with the preceding P26 in the NCOCX and NCOCA spectra. However, it could be unequivocally identified in the homonuclear DARR and CTUC−COCA spectra due to the well-resolved one-bond $C^{\alpha}-C^{\beta}$, $C^{\beta}-C^{\gamma}$, and $C^{\gamma}-C^{\delta 1}$ correlations. Finally, I87 is not present in the heteronuclear NCACB and NCACX data sets, but its ^{13}C peaks could be unambiguously assigned on the basis of the DARR spectra (as being the single remaining isoleucine residue after assignments of I36, I61, and I94), while its ^{15}N shift was inferred from the solution shift and from the N(i)−CO($i-1$)−CA($i-1$) cross-peak to the preceding G87 residue in the solid-state NCOCX data set. In summary, we have assigned 83 of 89 residues of CAP-Gly in the solid state.

We also note the superior resolution of the scalar-based 3D NCOCA and 2D NCO, NCA, and COCA−CACB data sets, consistent with the previous reports.[54,55,68] Due to the relatively low sensitivity of the 3D experiment because of the moderate MAS frequencies and moderate decoupling field strengths, cross-peaks for only 42 residues were present in the spectra; nevertheless, the spectra were critical for unambiguous assignments.

(68) Chen, L. L.; Olsen, R. A.; Elliott, D. W.; Boettcher, J. M.; Zhou, D. H. H.; Rienstra, C. M.; Mueller, L. J. *J. Am. Chem. Soc.* **2006**, *128*, 9992–9993.

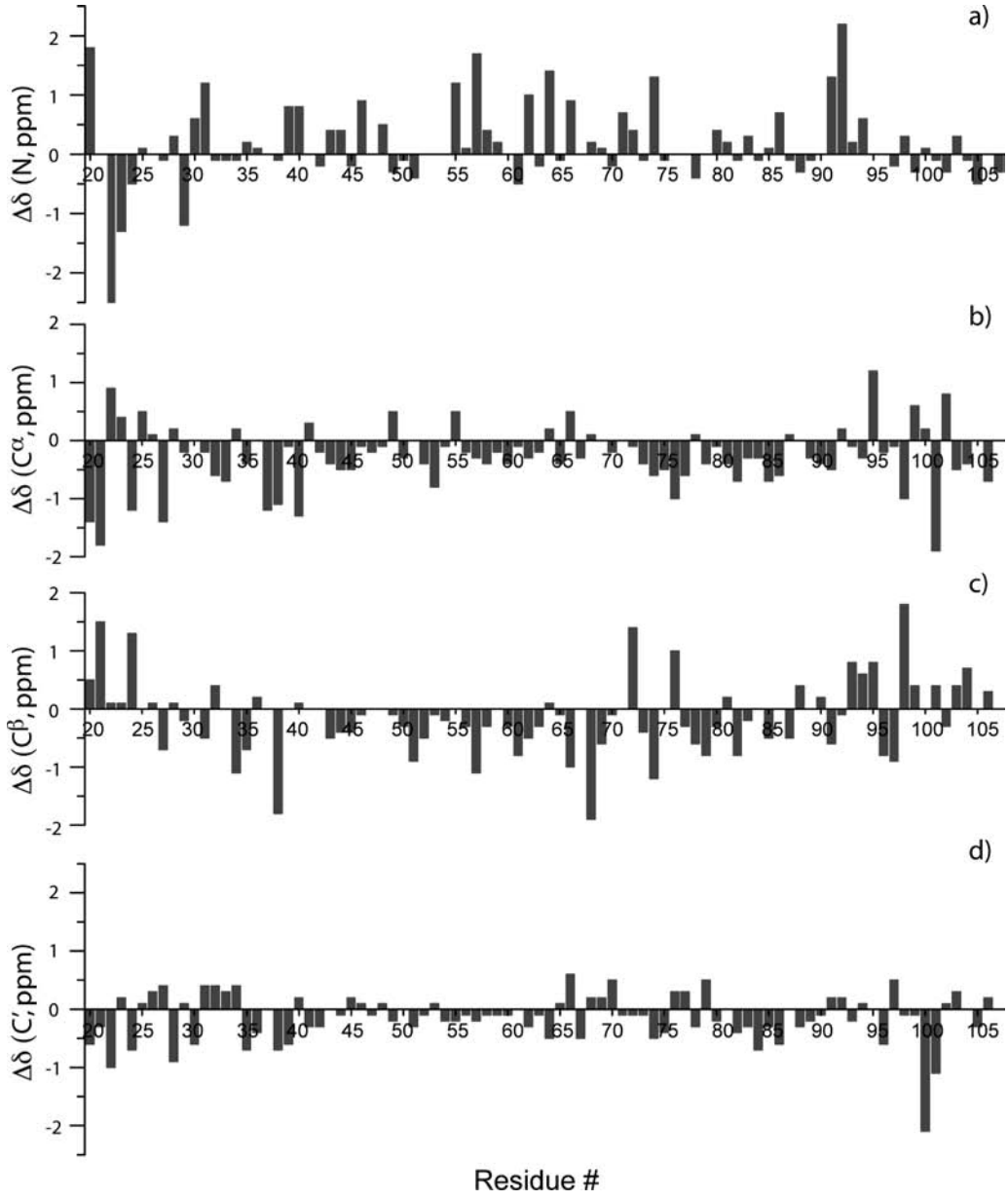

Figure 4. Differences between solid-state and solution chemical shifts plotted versus residue number in CAP-Gly for the backbone nitrogen and carbon atoms.

Examination of the ^{13}C and ^{15}N solid-state chemical shifts indicates that the majority of the residues are in a β-sheet conformation, consistent with solution NMR results. The solid-state chemical shifts are generally in very good agreement with the solution shifts (illustrated in Figure 4 and in the Supporting Information). We note that the general agreement between solid-state and solution chemical shifts has been observed in several prior reports, including our previous work on intact and reassembled thioredoxin[31–33] and BPTI[30] and work from other groups on Crh[37] and GB1.[45] Interestingly, in the case of CAP-Gly the differences between solid-state and solution chemical shifts are somewhat smaller than in the above proteins.

The TALOS analysis of the ψ and ϕ torsion angles on the basis of the solid-state chemical shifts summarized in Figure 5 reveals that the secondary structure of CAP-Gly in the solid state is generally consistent with both the solution and the X-ray crystallography results (see Figure S6 of the Supporting Information for comparison between the solid-state-NMR-derived torsion angles and those obtained from several X-ray structures of CAP-Gly). There are several residues for which deviations with the TALOS-predicted torsion angles from solid-state and solution shifts are observed: G42, A45, G55, L62, G71, D99-G100, T103-T104-S105. All of these residues but A45 are located in flexible loops or the termini of the individual secondary structure elements. Interestingly, the ψ torsion angle for A45 predicted by TALOS is consistent with the typical ψ value for a residue in a canonical β strand. In the crystal structures of CAP-Gly, A45 is located at the center of a twisted β strand, giving rise to an unusual ψ torsion angle, which is also well predicted from solution chemical shifts. The fact that TALOS could not reproduce this unusual ψ torsion angle is surprising in light of the fact that the chemical shift differences as measured by solid-state and solution NMR are generally small for all residues in the V44-A45-Y46 region (see Figure 4 and Table S4 of the Supporting Information). We therefore speculate

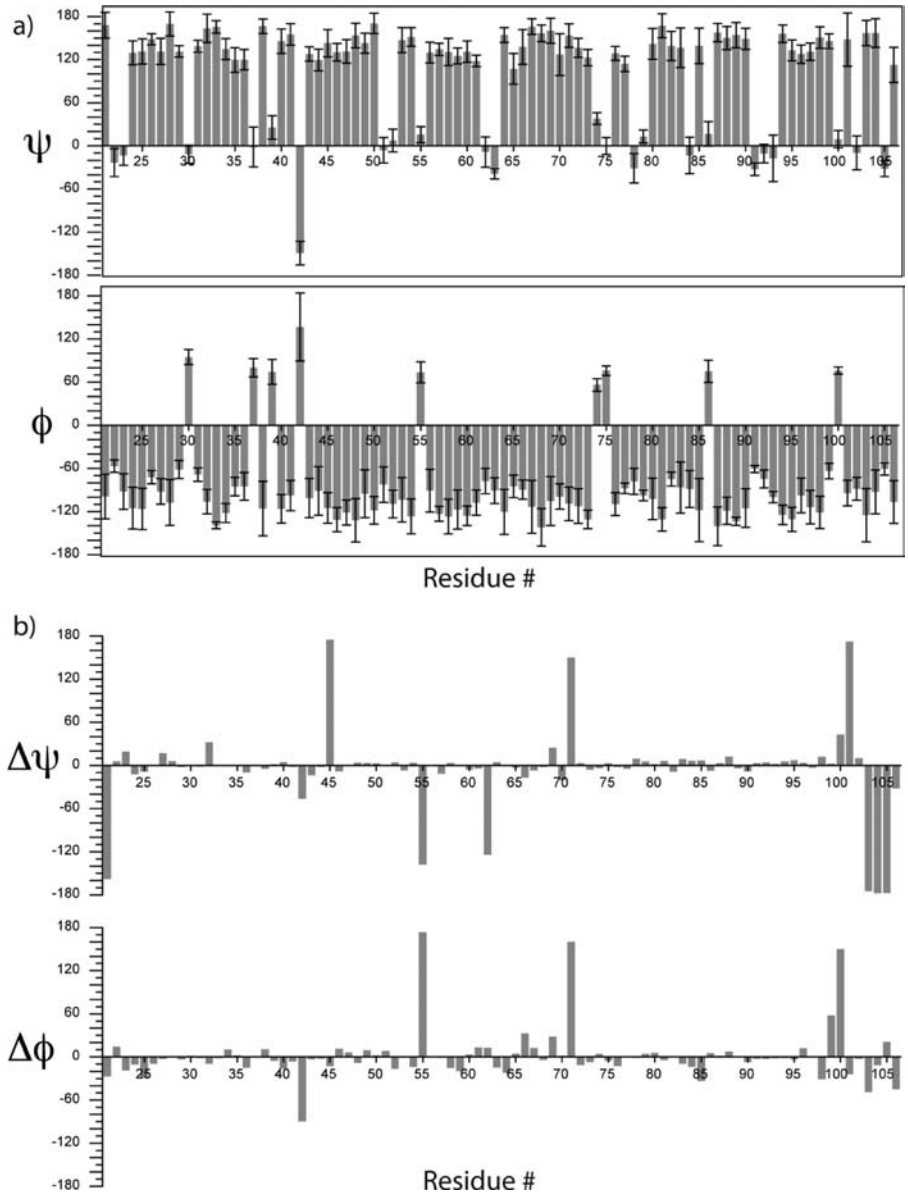

Figure 5. (a) Backbone torsion angles ψ (top) and ϕ (bottom) derived by TALOS[67] analysis of isotropic solid-state chemical shifts of CAP-Gly. (b) Differences in the backbone torsion angles $\Delta\psi$ (top) and $\Delta\phi$ (bottom) derived from the TALOS analysis of the solid-state and solution chemical shifts of CAP-Gly.

that TALOS failed to discern this structural nuance due to the lack of proton chemical shifts in the solid-state NMR data.

Characterization of CAP-Gly/Microtubule Binding. Cosedimentation. Tubulin was polymerized into microtubules upon incubation with paclitaxel and GTP (see the Experiments and Methods). Analysis of the pellet and the supernatant separated by ultracentrifugation revealed that most of the microtubules are in the pellet (Figure 6). For cosedimentation assay, varying amounts of CAP-Gly were added to the polymerized microtubules at pH 6 and 7 (see the Experiments and Methods). SDS−PAGE analysis of the pellet and supernatant indicates that a significant fraction of CAP-Gly is found in the pellet at both pH values and generally increases with an increase of the CAP-Gly:MT ratio (Figure 6). As illustrated in Figure 6, when 150 μM CAP-Gly and 10 μM tubulin dimer were used, ca. 30−35% of CAP-Gly was found in the pellet. Therefore, the CAP-Gly domain of the p150^{Glued} subunit of dynactin binds to microtubules in vitro under the conditions employed for NMR sample preparation. The control experiment reveals that, as expected, dynein light chain LC8 does not bind to microtubules, therefore corroborating that the CAP-Gly/MT interaction is specific. It is also estimated that the binding affinity between CAP-Gly and microtubules is in the micromolar range on the basis of a semiquantitative analysis of the cosedimentation assays conducted with varying CAP-Gly:MT ratios.

Electron Microscopy. Transmission electron microscopy (TEM) corroborated formation of stable microtubules under the experimental conditions, as anticipated (Figure 7A). TEM images of the CAP-Gly/MT complex (1:1 molar ratio) revealed that microtubules remain intact and suggested the presence of CAP-Gly on the MT surface (Figure 7B). However, no significant changes in the MT morphology were found, and no individual CAP-Gly molecules could be detected; therefore, we conclude that direct observation of CAP-Gly on the MT surface

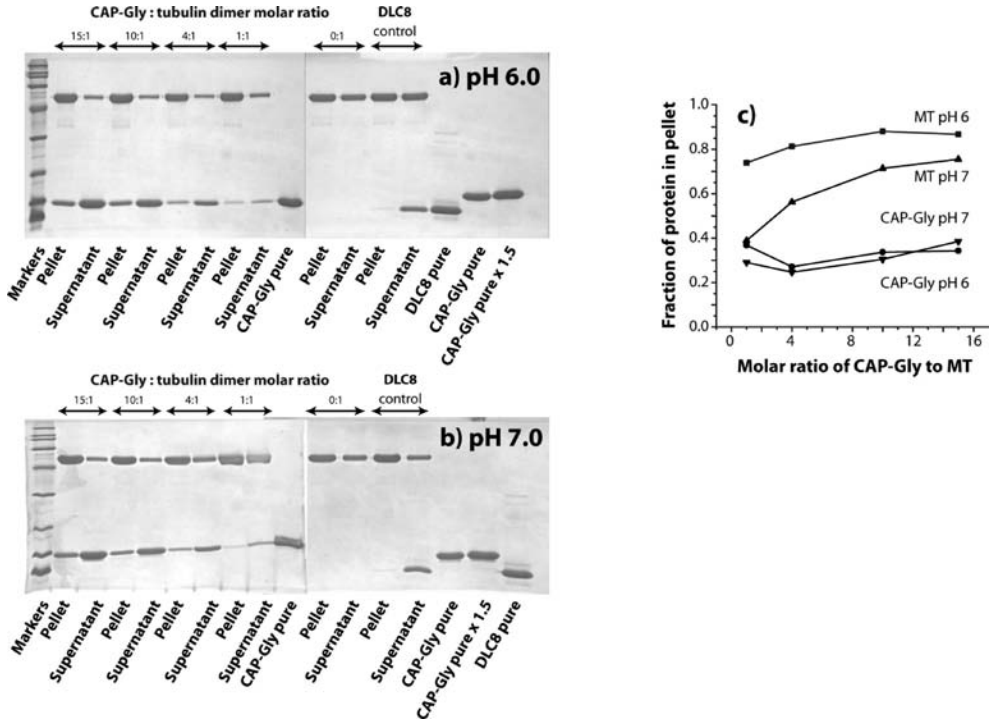

Figure 6. SDS−PAGE analysis of the CAP-Gly/microtubule interaction at pH 6.0 (a) and 7.0 (b). The cosedimentation assay conditions are described in the Experiments and Methods. (c) Fraction of the protein (CAP-Gly or microtubule) in the pellet as a function of the [CAP-Gly]:[tubulin] ratio.

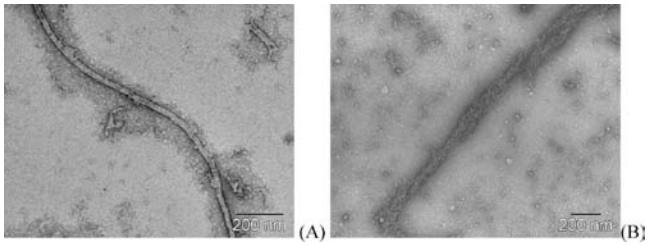

Figure 7. Transmission electron micrographs of the paclitaxel-stabilized microtubules free (A) and with CAP-Gly bound (1:1).

by transmission electron microscopy could not be accomplished under our experimental conditions.

Solution HSQC Spectroscopy of CAP-Gly Bound to Microtubules. To examine the binding of CAP-Gly to microtubules by solution NMR, we have performed HSQC titration experiments. Two sets of HSQC titrations were conducted for CAP-Gly/MT complexes. In one, the microtubule concentration was kept constant at 30 μM, and CAP-Gly was titrated into the solution to final concentrations of 30, 60, 120, 240, and 480 μM. As illustrated in Figure 8, with the exception of several residues belonging to the N- and C-termini, the peaks lose intensity. In another set of experiments, the CAP-Gly concentration was maintained constant at 480 μM while the microtubule concentration was systematically changed to 30, 15, 7.5, and 3.75 μM. As shown in Figure 8, at high CAP-Gly:MT ratios of 64:1 and 128:1 the peaks do not disappear but are broadened and lose intensity as the CAP-Gly:MT ratio decreases. The same behavior is observed at pH 7.0 (see Figure S7 of the Supporting Information). These results suggest that the motional flexibility of the terminal residues in the CAP-Gly/MT complex is retained, making the peaks observable while the resonances for the rest of the residues broaden or disappear due to the large molecular weight of the complex and/or possibly due to intermediate exchange, therefore precluding any site-specific analysis of the CAP-Gly interactions with the microtubules under the experimental conditions.

HSQC spectra were also acquired for an additional CAP-Gly/MT sample prepared at pH 7.0 and consisting of the supernatant separated from the centrifuged CAP-Gly/MT mixture where the pellet was used for the solid-state NMR experiments (see the Experiments and Methods). On the basis of the semiquantitative estimates from the cosedimentation assay, the supernatant contains 150 μM CAP-Gly and 3.85 mM MT. The HSQC spectra revealed weak but distinct chemical shift perturbations for several residues: H40, T43, D63, E64, A65, K66, G71, G84, and Q95 (illustrated in Figure 9). Similar behavior in the HSQC spectra is observed when CAP-Gly is mixed with nonpolymerized tubulin at three different ratios (see the Experiments and Methods, spectra shown in Figure S7 of the Supporting Information), indicating that the chemical shift perturbations for select residues of CAP-Gly in the above samples correspond to binding of the protein to unpolymerized tubulin or to relatively small tubulin oligomers rather than to polymeric microtubules. Therefore, the molecular weight of these CAP-Gly/tubulin complexes must be relatively small, permitting observation of binding-induced chemical shift changes. We note that the chemical shift perturbations observed in the presence of tubulin correspond to the residues located on the surface in the vicinity of the highly conserved ^{67}GKND^{71} motif. The full structural characterization of the CAP-Gly bound to microtubules using solid-state NMR spectroscopy will address whether these residues represent the CAP-Gly/MT interface.

Solid-State DARR Spectra of CAP-Gly Bound to Microtubules. To determine the optimal experimental conditions for solid-state NMR analysis of CAP-Gly bound to microtubules, we have examined the temperature dependence of the 2D DARR spectra of the complex. In striking contrast to the free protein, the ^{13}C cross-polarization signal is very weak at temperatures above −15 °C, and no signal could be detected above 0 °C.

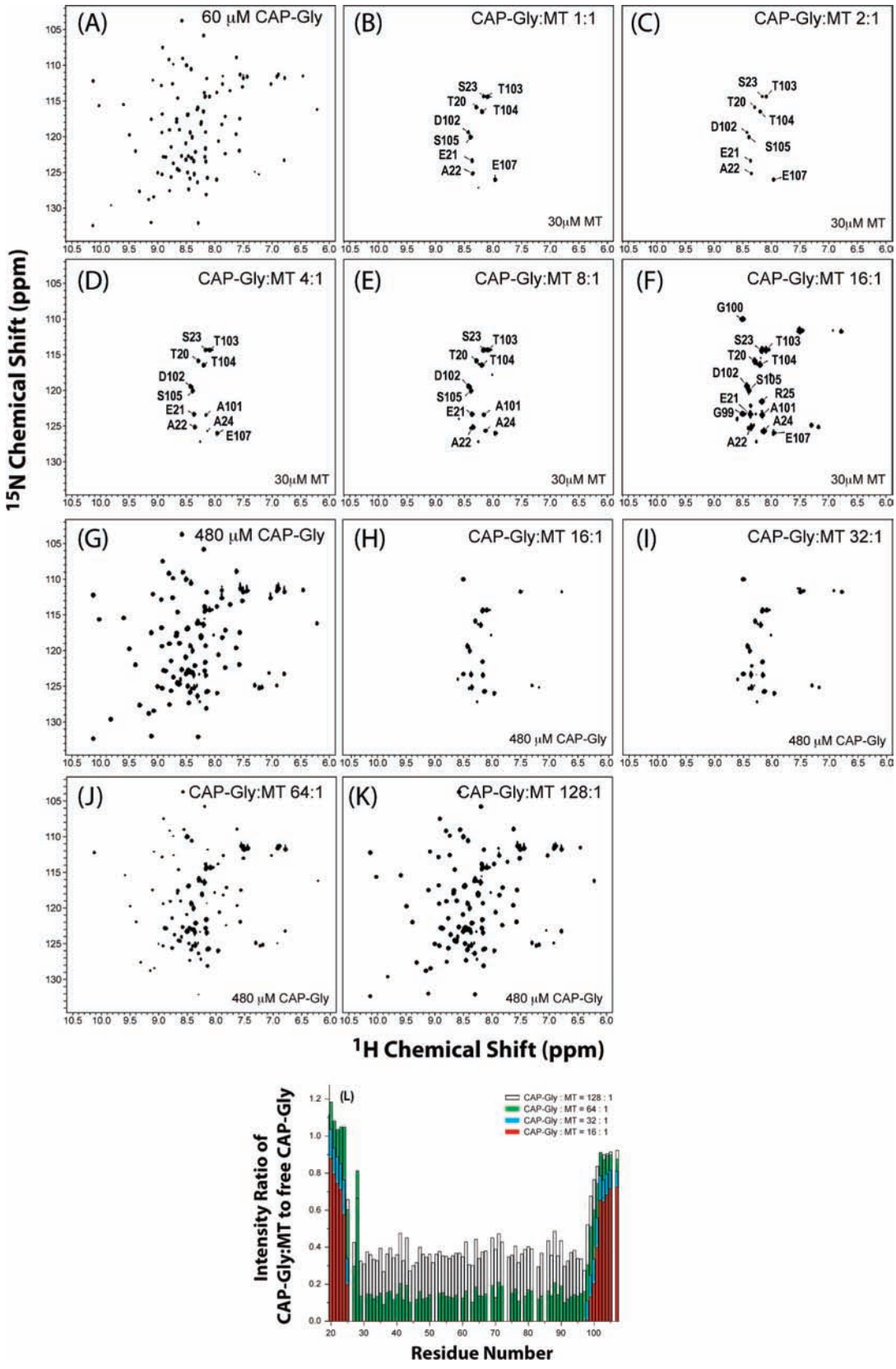

Figure 8. (A−J) Solution HSQC titration experiments. Spectra A and G are HSQC spectra of free CAP-Gly at pH 6.0 (60 and 480 μM, respectively). Spectra B−F represent titration experiments where the concentration of microtubules was kept constant at 30 μM and CAP-Gly was added to final [CAP-Gly]:[MT] ratios of 1:1, 2:1, 4:1, 8:1, and 16:1, respectively. Spectra H−K represent titration experiments where the concentration of CAP-Gly was kept constant at 480 μM and the concentration of the microtubules was varied to final [CAP-Gly]:[MT] ratios of 16:1, 32:1, 64:1, and 128:1, respectively. (L) Intensities of the peaks in the HSQC spectra versus residue number for different [CAP-Gly]:[MT] ratios: 128:1 (white), 64:1 (green), 32:1 (blue), 16:1 (red).

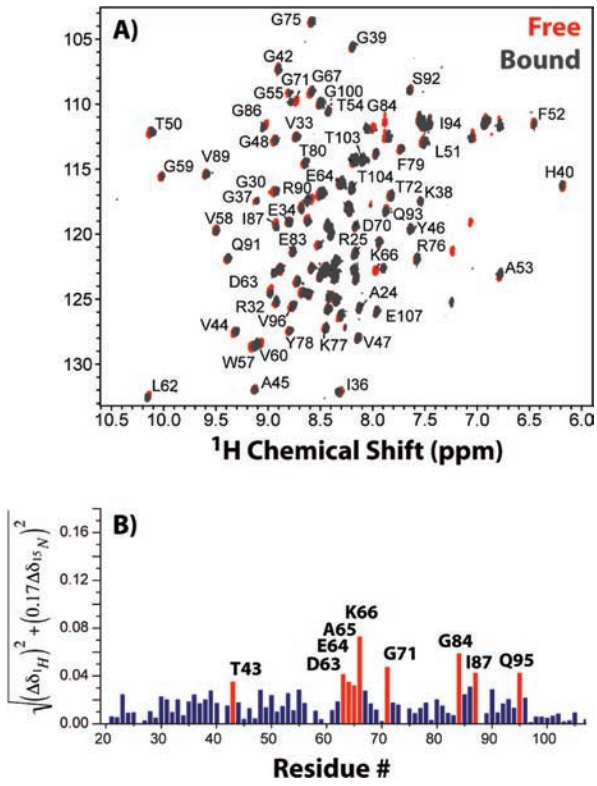

Figure 9. (A) Overlay of the HSQC spectra of CAP-Gly at pH 7.0 in the free form (red) and in the presence of short microtubule fragments (dark gray). (B) Weighted chemical shift changes versus residue number in CAP-Gly upon binding to the microtubule fragments.

The ^{13}C cross-polarization signal intensity increases with lowering of the temperature. We have therefore chosen to perform all solid-state NMR experiments of the CAP-Gly/MT complex at −38.2 °C, the lowest temperature that could be maintained stably on the 21.1 T instrument under our experimental conditions. What gives rise to the decrease in CP efficiency and the eventual disappearance of the signal as the temperature is increased is not clear at present. We note that at temperatures above the freezing point the sample has gel consistency, and we speculate that under those conditions microtubules might be flexible and conformationally heterogeneous, resulting in turn in conformational heterogeneity of bound CAP-Gly. Molecular-level understanding of this interesting behavior will require additional experiments, which are beyond the scope of this work and will be pursued in the future.

The 21.1 T DARR spectra of the CAP-Gly/MT complex at −38.2 °C exhibit well-resolved lines with the width of the individual cross-peaks on the order of 0.5−0.8 ppm (Figure 10). These line widths are comparable to or somewhat broader than those in the free protein; whether this is an inherent characteristic of the sample is not clear as lower temperatures (where the lines might be narrower) were not accessible. Nevertheless, a large number of resolved peaks are present in the data, allowing for the analysis of chemical shifts in the complex with respect to the free CAP-Gly.

In Figure 10, the DARR spectra of the CAP-Gly/MT complex and the free CAP-Gly are compared. Remarkably, chemical shifts for a significant number of residues are perturbed upon formation of the complex. While some of the chemical shift changes are 0.1−0.3 ppm and could possibly be accounted for by the different temperatures at which the spectra of the free protein and the complex had to be recorded, the shifts differ by 0.5 ppm or more in many residues, which is clearly not due to temperature variations alone (vide supra). These large chemical shift perturbations are likely due to conformational changes in CAP-Gly upon CAP-Gly/MT complex formation. While complete resonance assignments of the DARR spectra of the complex are not possible in the absence of a complete set of 3D homo- and heteronuclear spectra, partial analysis of the spectra was performed for the outlier cross-peaks. In Table 1, chemical shifts of C^{α} and C^{β} carbons in selected residues of free and bound CAP-Gly are illustrated. Two interesting observations can be made from this analysis. First, chemical shift perturbations occur in the entire CAP-Gly molecule, rather than in a specific contiguous stretch of residues. These changes indicate that the backbone torsion angles are different between the free and MT-bound CAP-Gly. Second, the absolute magnitude of these chemical shift perturbations is such that the overall secondary structure of the corresponding residues does not change. In aggregate, these results suggest that multiple small conformational rearrangements take place throughout the protein upon its binding to microtubules. To gain atomic-resolution insight into these structural rearrangements upon binding, full resonance assignments of the CAP-Gly assembled on the microtubules are needed.

The DARR spectra of the CAP-Gly/MT complex presented in this work were acquired with only 1−2 mg of CAP-Gly in the sample, resulting in limited sensitivity of the measurements and precluding the collection of heteronuclear correlation spectra. Therefore, detailed structural analysis of the bound CAP-Gly was not feasible from the present data sets. Nevertheless, the current results demonstrate that CAP-Gly/MT complexes give rise to high-resolution MAS spectra, and with improved sample preparation protocols complete structural characterization of these assemblies will be possible. This work is currently under way.

Discussion

Atomic-level structural analysis of interactions between the CAP-Gly domain of the $p150^{Glued}$ subunit of dynactin and fragments of other microtubule plus end tracking proteins such as EB1 and CLIP-170 have provided insight into the biological role of $p150^{Glued}$ CAP-Gly in the complex multicomponent network at the plus end of the microtubule.[26–29] These studies employed X-ray crystallography and/or solution NMR spectroscopy, as well as various biophysical methods. These approaches however are difficult to utilize in structural investigations of microtubule-associated proteins bound to microtubules because of the intrinsic insolubility and lack of long-range order in these systems, and their large size. At the same time, direct atomic-level knowledge about the structure and dynamics of CAP-Gly/MT assemblies is needed to fully understand the role of CAP-Gly and its relationship to the different functions of dynactin. The studies of the CAP-Gly domain of dynactin interacting with microtubules reported here represent the first step toward establishing such insight.

While solution NMR methods provided detailed information on the Tau/MT interaction,[69] similar methods were unable to provide site-specific insight for the CAP-Gly/MT interaction. This may simply reflect the fact that Tau is predominantly disordered in the MT-free state and makes a large number of

(69) Sillen, A.; Barbier, P.; Landrieu, I.; Lefebvre, S.; Wieruszeski, J. M.; Leroy, A.; Peyrot, V.; Lippens, G. *Biochemistry* **2007**, *46*, 3055–3064.
(70) Mossessova, E.; Lima, C. D. *Mol. Cell* **2000**, *5*, 865–876.
(71) Marley, J.; Lu, M.; Bracken, C. *J. Biomol. NMR* **2001**, *20*, 71–75.

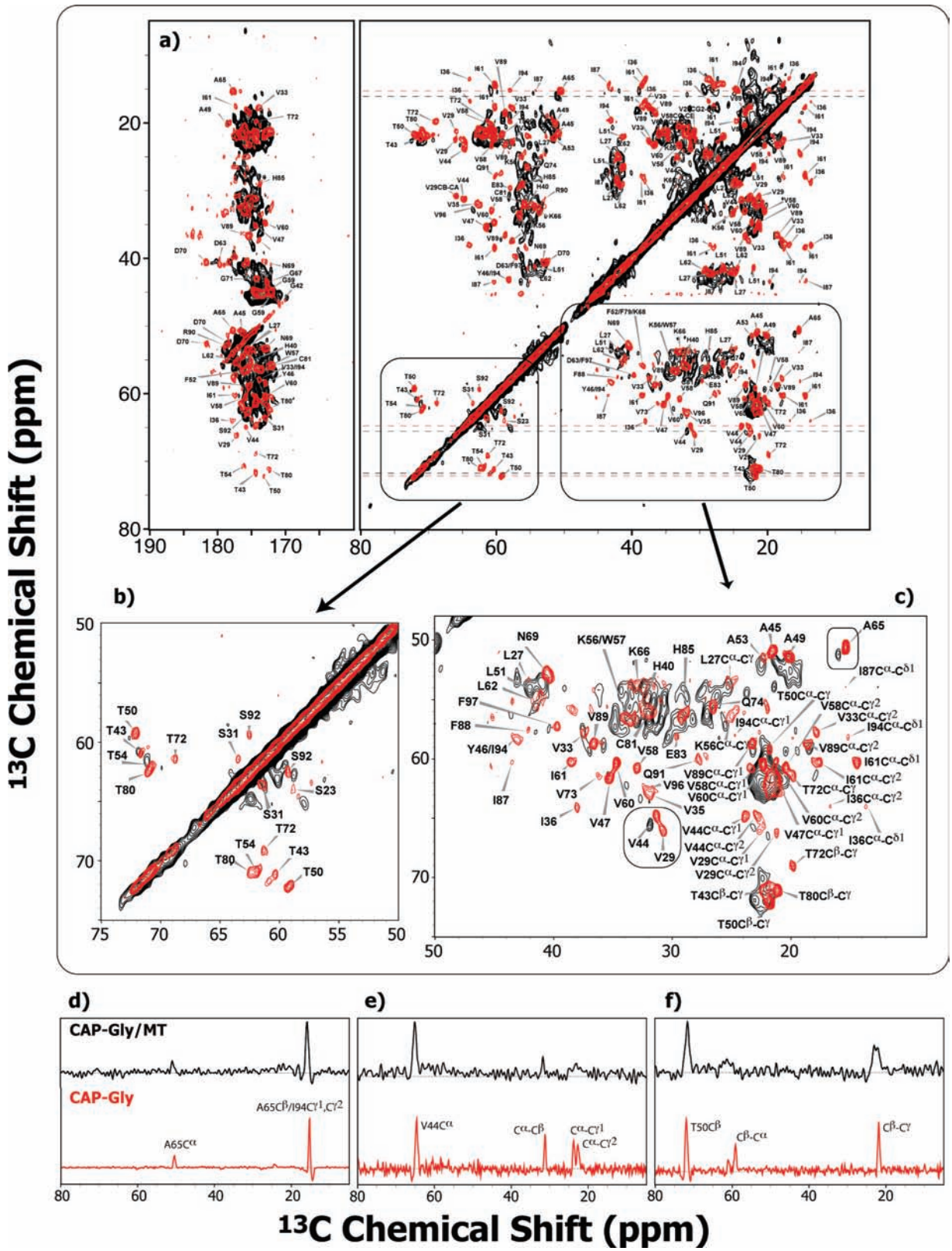

Figure 10. DARR spectra (21.1 T) of the CAP-Gly/MT complex (black) overlaid with the spectra of the free CAP-Gly (red): aliphatic and carbonyl regions (a) and expansions of the aliphatic regions (b, c) illustrating the chemical shift differences in CAP-Gly upon binding to microtubules. The spectra of the complex were acquired at −38.2 °C. The first contour is set at 4σ with a level multiplier of 1.2. In (b) and (c), the labels refer to the $C^{\alpha}-C^{\beta}$ correlations for specific residues unless indicated otherwise. The dashed lines in (a) correspond to the representative slices drawn through the aliphatic regions of DARR spectra and illustrating the cross-peaks for A65 (d), V44 (e), and T50 (f). These slices are color coded red for the free CAP-Gly and black for the CAP-Gly bound to microtubules.

contacts in the MT-bound state whereas CAP-Gly is predominantly folded in solution and presumably in the MT-bound state. Nonetheless, we did detect small chemical shift perturbations in several specific residues for one of the CAP-Gly/MT samples.

Table 1. ^{13}C Chemical Shifts (ppm) for Selected Residues in Free CAP-Gly and in the CAP-Gly/MT Complex from 2D 21.1 T DARR Spectra

	free CAP-Gly		CAP-Gly/MT complex	
residue	C^{α}	C^{β}	C^{α}	C^{β}
T43	60.4	71.6	60.7	71.9
T50	59.1	72.1	59.7	72.5
T80	62.4	70.9	64.0	70.4
S23	58.6	64.0	58.0	65.1
S31	61.1	63.5	62.4	65.0
A65	50.6	15.4	51.3	16.0
V44	64.7	31.1	65.6	31.9

This most likely indicates that the sample consists of shorter oligomeric MT fragments or tubulin dimers, as evidenced by similar results when nonpolymerized tubulin was employed. In contrast, for the CAP-Gly/MT preparations containing polymeric microtubule structures, we have observed that most of the CAP-Gly signals with the exception of those belonging to several terminal residues are severely broadened by the loss of mobility in a high molecular weight complex and/or due to chemical exchange broadening, rendering them undetectable even when the CAP-Gly concentration is 480 μM and the CAP-Gly:MT ratio is 32:1. On the contrary, free CAP-Gly shows very well resolved spectra with all peaks readily observable. We therefore conclude that solution NMR alone is not sufficient for gaining the atomic-level structural information in the CAP-Gly/MT complex.

In contrast, solid-state MAS NMR spectroscopy has no intrinsic limitations for the size of the protein under investigation and thus provides an alternative method for structural studies of CAP-Gly/MT assemblies. We have observed distinct temperature dependence of the DARR spectra in the free protein and of the complex. The DARR $^{13}C-^{13}C$ correlation spectrum of the CAP-Gly/MT complex is well resolved at low temperatures, indicating that site-specific resonance assignments will be possible with heteronuclear correlation spectroscopy and that amino acid residues of CAP-Gly which are involved in the CAP-Gly/MT interaction can be directly inferred from chemical shift analysis once the assignments are completed. We have already observed in the solid-state DARR spectra substantial chemical shift perturbations for a number of residues upon binding of CAP-Gly to microtubules, suggesting conformational changes may be taking place in CAP-Gly upon formation of the complex. Interestingly, while these chemical shift differences are significant, ranging between 0.3 and 1.5 ppm for carbon atoms in various CAP-Gly residues (see Table 1) and indicating changes in backbone torsion angles upon binding, the shifts of the MT-bound protein suggest that the overall secondary structure is preserved. These results suggest that, upon binding to microtubules, CAP-Gly may experience multiple small conformational rearrangements. Detailed atomic-level insight into these structural changes in the MT-bound CAP-Gly remains to be gained and will require full resonance assignments of the bound protein; this is the subject of our ongoing studies.

The current results thus indicate that the structure and dynamic behavior of CAP-Gly are sensitive to the interactions with the microtubules and open exciting opportunities for detailed structural studies of these assemblies by solid-state NMR spectroscopy.

Experiments and Methods

Materials. Common chemicals were purchased from Fisher Scientific or Sigma-Aldrich. Bovine brain tubulin was purchased from Cytoskeleton, Inc. and used for microtubule polymerization in vitro without purification. GTP was purchased from MP, and paclitaxel was purchased from Alexis. $^{15}NH_4Cl$ and U-$^{13}C_6$ glucose were purchased from Cambridge Laboratories, Inc. Copper grids (400 mesh) coated with Formval and stabilized with evaporated carbon films were purchased from Electron Microscopy Sciences. The SMT3 fusion vector and Ulp1 protease expression system[70] was a generous gift of Dr. Christopher Lima (Weill Medical College, Cornell University).

Expression and Purification of Isotopically Enriched CAP-Gly. The CAP-Gly domain of the p150^{Glued} subunit of mammalian dynactin encompassing residues 19−107 was subcoloned into the pET28b-His6-SMT3 vector[70] using *Bam*HI and *Xho*I restriction sites. DNA sequencing confirmed successful subcloning. The (SMT-His6)-CAP-Gly was transformed into *Escherichia coli* BL21(DE3) cells. To prepare natural abundance CAP-Gly, 1 L of *E. coli* cultures with (SMT-His6)-CAP-Gly was grown in rich LB medium at 37 °C to 0.5 OD^{600} and induced with 250 μM IPTG at 37 °C for 3 h. To prepare uniformly $^{13}C/^{15}N$ enriched CAP-Gly, an expression protocol developed by Bracken was employed.[71] Cells were grown in 1 L of LB medium to 0.7 OD^{600}, then harvested by centrifugation (RCF 4000*g*, 30 min), washed with M9 medium depleted of carbon and nitrogen source, and centrifuged again. Cell pellets were resuspended with 250 mL of M9 medium containing $^{15}NH_4Cl$/U-$^{13}C_6$ glucose. Protein expression was induced with 0.8 mM IPTG for 4 h after 1 h of recovery at 37 °C.

Cells containing the protein were harvested, lysed, and clarified. The soluble (SMT-His_6)-CAP-Gly was purified by Ni affinity chromatography (HisTrap HP, GE Healthcare). The fractions containing the target protein were treated with (His_6)-ULP-1 enzyme to cleave the His-SMT tag. CAP-Gly$^{(19-107)}$ was then separated from His_6-SMT3 and His_6-ULP-1 by Ni affinity chromatography. The CAP-Gly fractions were combined and further purified by anion exchange (HiTrap FF-Q, GE Healthcare) chromatography to remove the residual protein and nucleic acid impurities. A 12 mg portion of pure $^{15}N/^{13}C$-labeled CAP-Gly is typically generated per 1 L of LB medium/250 mL of M9 medium. The yield of the natural abundance CAP-Gly is 22 mg/L of LB medium.

Biochemical characterization of CAP-Gly was performed to assess its stability and hydrodynamic properties. Sedimentation equilibrium experiments through analytical ultracentrifugation show that the protein is monomeric. Thermal denaturation of the CAP-Gly using circular dichroism to follow secondary structure changes shows that the protein is stable with $T_M = 60$ °C; additional details are presented in the Supporting Information (see Figures S8 and S9 together with the corresponding text).

Preparation of Paclitaxel-Stabilized Microtubules. Paclitaxel-stabilized microtubules were assembled using the protocol described by Sillen.[69] Tubulin was diluted in 25 mM phosphate buffer containing 25 mM NaCl, 8 mM $MgCl_2$, and 0.4 mM DTT, pH 6 or 7. Typically, 30 μM tubulin, 0.1 mM GTP, and 15 μM paclitaxel were incubated at 37 °C for 40−45 min. Microtubule assembly experiments at higher starting concentrations of tubulin were successful as well. Microtubules stabilized by paclitaxel were diluted to desired concentrations for cosedimentation assays, electron microscopy study, and NMR experiments.

Cosedimentation Assay and SDS−PAGE Analysis of CAP-Gly/Microtubule Complexes. To assess the binding of CAP-Gly to paclitaxel-stabilized microtubules, solutions containing varying ratios of CAP-Gly to microtubules were prepared by mixing CAP-Gly and freshly polymerized microtubules. The dynein light chain DLC8/DynLL1 was used as a control in a separate experiment to corroborate lack of nonspecific binding. These samples contained

(72) Wishart, D. S.; Bigam, C. G.; Yao, J.; Abildgaard, F.; Dyson, H. J.; Oldfield, E.; Markley, J. L.; Sykes, B. D. *J. Biomol. NMR* **1995**, *6*, 135–40.
(73) Baldus, M.; Petkova, A. T.; Herzfeld, J.; Griffin, R. G. *Mol. Phys.* **1998**, *95*, 1197–1207.

10 μM microtubules and various concentrations of CAP-Gly (0, 10, 40, 100, and 150 μM). The DLC8/MT control contained 36 μM DLC8 and 10 μM microtubules. Other controls contained 176 μM CAP-Gly or 90 μM DLC8 only. The volume of all samples and controls was 50 μM. These samples and controls were centrifuged in an Eppendorff 5424 microcentrifuge (RCF 21000g, 40 min). The supernatant was separated from the pellet, and the pellet was suspended in 50 μL of phosphate buffer. A 25 μL portion of each sample was mixed with 25 μL of 2× SDS sample buffer, and 12 μL of the mixture was loaded onto 15% acrylamide gel for SDS−PAGE analysis except for one well onto which 18 μM pure CAP-Gly was loaded as a control sample for quantification of the protein amount. The protein amount was quantified with the BioRad Quantity One software package.

Electron Microscopy. Paclitaxel-stabilized microtubules and their complexes with CAP-Gly were analyzed in a Zeiss CEM 902 transmission electron microscope operating at 80 kV. Samples were stained with ammonium molybdate (5%, w/v), deposited onto 400 mesh, Formval/carbon-coated copper grids, and dried. For the microtubules alone, the concentration was 5 μM. For the CAP-Gly/MT complexes, the concentrations of both CAP-Gly and MT were 5 μM. The magnification ratios for MT and CAP-Gly/MT complexes were 80 000 and 50 000, respectively.

Preparation of NMR Samples. For solution NMR spectroscopy of free CAP-Gly, 500 μL of 0.96 mM [U-^{15}N,^{13}C]CAP-Gly were prepared in 20 mM phosphate buffer, pH 6.0 (50 mM NaCl, 1 mM DTT, and 0.3% NaN_3). Another U-^{15}N,^{13}C-labeled CAP-Gly sample was prepared in 20 mM phosphate buffer, pH 7.0, and also used for solution NMR resonance assignments.

For the study of CAP-Gly/MT interaction in solution, [U-^{15}N]CAP-Gly was concentrated to 14.1 mg/mL (1.48 mM) and diluted to the desired concentrations by adding varying amounts of paclitaxel-stabilized microtubules and/or the same tubulin polymerization buffers (pH 6 and 7) used for microtubule assembly (see above). Additionally, three samples were prepared for studies of interactions of CAP-Gly with nonpolymerized tubulin at pH 7.0 (the tubulin polymerization buffer; see above); the final solutions contained [U-^{15}N]CAP-Gly (150 μM) and unpolymerized tubulin (3.85, 10.75, and 20 μM).

A sample of free CAP-Gly for solid-state NMR studies was prepared by controlled precipitation from polyethylene glycol by slow addition of a solution of 32% PEG-3350 to the solution of 13.9 mg of CAP-Gly (27 mg/mL), both dissolved in 10 mM MES buffer (10 mM $MgCl_2$, pH 6.0), following the protocol developed previously for thioredoxin.[31] This condition was chosen from a minimal hanging drop screen and yields CAP-Gly microcrystals in a hanging drop. The sample was centrifuged, the supernatant removed, and the pellet used for solid-state NMR experiments. More than 95% protein was found to be precipitated as indicated by the Bradford assay. A 14.2 mg portion of hydrated precipitate was packed into a 3.2 mm Varian rotor which was sealed using an upper spacer and a top spinner.

A sample of the CAP-Gly/microtubule complex for solid-state NMR studies was prepared by cosedimentation of 1.5 mL of 7.3 mg/mL CAP-Gly with 3.165 mL of 23 μM paclitaxel-stabilized microtubules (the final concentration was 247 μM for CAP-Gly and 15.6 μM for MT, and the CAP-Gly:MT molar ratio was 15.8:1). The resulting complex was centrifuged in a Sorvall Discovery 90 ultracentrifuge T865 rotor (RCF 80000g, 40 min), and 14.2 mg of hydrated gel-like pellets were transferred into a 3.2 mm Varian rotor which was sealed using an upper spacer and a top spinner. On the basis of SDS−PAGE analysis of the cosedimentation assay (see the Results), the sample contains a total of 1.2−2 mg of CAP-Gly. The supernatant was taken for solution NMR study (see the Supporting Information).

NMR Spectroscopy. Solution NMR spectra of U-^{15}N,^{13}C-labeled CAP-Gly were acquired at 14.1 T (600 MHz) on a Bruker Avance spectrometer outfitted with a triple-resonance inverse detection probe; Larmor frequencies were 600.133 MHz for ^{1}H, 150.9 MHz for ^{13}C, and 60.8 MHz for ^{15}N. HNCA, CBCA(CO)NH, HNCO, HN(CA)CO, and HBHA(CO)NH triple-resonance experiments were performed to obtain sequential backbone resonance assignments. All experiments were conducted at 298 K. Chemical shifts were referenced to DSS.[72] Detailed acquisition and processing parameters for each triple-resonance experiment are given in the Supporting Information.

Solid-state NMR spectra were acquired at 14.1 T (600 MHz) on a narrow Varian InfinityPlus instrument outfitted with a 3.2 mm triple-resonance T3 probe; Larmor frequencies were 599.5 MHz for ^{1}H, 150.7 MHz for ^{13}C, and 60.7 MHz for ^{15}N. Dipolar-based two- and three-dimensional DARR, NCA, NCO, NCACB, and NCOCX spectra were collected at an MAS frequency of 10.000 ± 0.001 kHz controlled by a Varian MAS controller; an additional set of DARR spectra was acquired at an MAS frequency of 14.705 kHz. The dipolar NCOCX experiment utilized the SPECIFIC-CP heteronuclear mixing[73] followed by the DARR mixing sequence;[74] in the NCACB experiment the homonuclear DREAM mixing[75] with a tangent ramp was used. Scalar-based two- and three-dimensional CTUC−COCA, CTUC−CACB, and NCOCA spectra[54,55,68] were collected at an MAS frequency of 14.705 kHz. The MAS frequency was controlled to within ±1 Hz by a Varian controller. The temperature was calibrated for this probe at different MAS frequencies using a $PbNO_3$ temperature sensor,[76] and the actual temperature at the sample was maintained to within ±0.5 °C throughout the experiments using the Varian temperature controller. The DARR spectra were acquired at temperatures of −1.7, −11.7, −16.7, and −34.9. The heteronuclear 2D and 3D spectra were acquired at −16.7 °C. ^{1}H, ^{13}C, and ^{15}N chemical shifts were referenced with respect to external referencing standards DSS, adamantane, and ammonium chloride.[77] The typical pulse lengths in the double-resonance mode were 2.6 μs (^{1}H) and 3.1 μs (^{13}C); the pulse lengths in the triple-resonance mode were 2.6 μs (^{1}H), 5 μs (^{13}C), and 5 μs (^{15}N). The ^{1}H−^{13}C(^{15}N) cross-polarization was performed with a tangent amplitude ramp (80−100%); the ^{1}H radio frequency field was 50 kHz with the center of the ramp Hartmann−Hahn matched to the first spinning sideband. The ^{1}H−^{13}C and ^{1}H−^{15}N contact times were 850 μs and 1.1 ms, respectively. The Z-filter time was 30 ms in all J-based experiments. In the dipolar-based experiments, DARR mixing times were 2 and 10 ms, the SPECIFIC-CP mixing times were 6.7 ms, and the DREAM mixing time was 2.05 ms. In the scalar-based COCA and CACB experiments, the rotor-synchronized delays were $\tau_1 = 4.080$ ms and $\tau_2 = 2.720$ ms. In the scalar-based NCO experiment, $\tau_1 = \tau_2 = 11.2$ ms; in the NCA experiment, $\tau_1 = 11.2$ ms and $\tau_2 = 6.12$ ms. In the scalar-based NCOCA experiment, $\tau_1 = \tau_2 = 11.2$ ms and $\tau_3 = \tau_4 = 2.72$ ms. TPPM decoupling[78] was used, and the decoupling field strengths ranged between 80 and 100 kHz in different experiments. Recycle delays in all experiments were 2 s. TPPI[79] was used for frequency discrimination in the indirect dimensions.

(74) Takegoshi, K.; Nakamura, S.; Terao, T. *Chem. Phys. Lett.* **2001**, *344*, 631–637.
(75) Verel, R.; Baldus, M.; Ernst, M.; Meier, B. H. *Chem. Phys. Lett.* **1998**, *287*, 421–428.
(76) Neue, G.; Dybowski, C. *Solid State Nucl. Magn. Reson.* **1997**, *7*, 333–336.
(77) Morcombe, C. R.; Zilm, K. W. *J. Magn. Reson.* **2003**, *162*, 479–486.
(78) Bennett, A. E.; Rienstra, C. M.; Auger, M.; Lakshmi, K. V.; Griffin, R. G. *J. Chem. Phys.* **1995**, *103*, 6951–6958.
(79) Marion, D.; Wuthrich, K. *Biochem. Biophys. Res. Commun.* **1983**, *113*, 967–74.
(80) Delaglio, F.; Grzesiek, S.; Vuister, G. W.; Zhu, G.; Pfeifer, J.; Bax, A. *J. Biomol. NMR* **1995**, *6*, 277–293.
(81) Goddard, T. D.; Kneller, D. G. Sparky 3. University of California, San Francisco.

DARR spectra of free CAP-Gly and of the CAP-Gly/MT complex were also acquired at 21.1 T on a medium-bore Varian Inova instrument outfitted with a 3.2 mm triple-resonance BioMAS probe; the Larmor frequencies were 900.575 MHz for ^{1}H and 226.47 MHz for ^{13}C. The MAS frequency was 14.000 ± 0.001 kHz controlled by a Varian MAS controller. The temperature was maintained to within ±0.5 °C throughout the experiments using the Varian temperature controller; for the free sample the temperature was −15 °C, and for the CAP-Gly/MT complex it was −38.2 °C. The pulse lengths in the DARR experiments were 3.8 s (^{1}H) and 6.3 μs (^{13}C); the ^{1}H−^{13}C cross-polarization was performed with a tangent amplitude ramp (80−100%). The ^{1}H radio frequency field was 68 kHz with the center of the ramp Hartmann−Hahn matched to the second spinning sideband; the ^{1}H−^{13}C contact time was 1 ms. TPPM decoupling (71 kHz) was applied during the evolution and acquisition periods. The ^{1}H field strength during DARR was 14 kHz; DARR mixing time was 50 ms. Under these conditions predominantly one-bond correlations appear in the spectra.

The pulse sequences for 2D and 3D MAS experiments conducted for resonance assignments are shown in Figure S10 of the Supporting Information. Other acquisition parameters for data sets acquired at 14.1 and 21.1 T are specified in the figure captions and in Table S5 of the Supporting Information.

NMR Data Processing and Analysis. The spectra were processed in NMRpipe[80] and analyzed in Sparky.[81] For 2D solid-state NMR data, 90°, 60°, or 30° shifted sine bell apodization followed by a Lorentzian-to-Gaussian transformation was applied in both dimensions; forward linear prediction to twice the number of the original data points was employed in the indirect dimension for some data sets followed by zero filling to twice the total number of points. The 3D data sets were processed by using 30° or 60° shifted sine bells in all dimensions followed by a Lorentzian-to-Gaussian transformation (for resolution enhancement) and by using 90° shifted sine bells in all dimensions followed by a Lorentzian-to-Gaussian transformation (for sensitivity enhancement). The 3D spectra were also processed with maximum entropy reconstruction as implemented in the program Roland NMR Toolkit.[82,83] Detailed information about processing parameters is specified in Table S5 of the Supporting Information. Backbone torsion angles were predicted in TALOS[67] on the basis of isotropic solution ^{1}H, ^{13}C, and ^{15}N or solid-state ^{13}C and ^{15}N chemical shifts and without manual optimization against existing published structures.

Conclusions

In summary, we have employed a combination of solid-state and solution NMR spectroscopy to study the CAP-Gly domain of mammalian dynactin and its interactions with microtubules. Free CAP-Gly exhibits well-resolved lines both in solution and in the solid state and is amenable to detailed structural characterization. Analysis of chemical shifts based on the site-specific resonance assignments in solution and in the solid state reported here indicates that the secondary structure of the protein is predominantly β-sheet, and backbone torsion angles predicted by TALOS are in very good agreement with X-ray structures of CAP-Gly reported previously, with the exception of the residues located in flexible loops or at the termini of the individual secondary structure elements. The conventional chemical shift perturbation approach by solution NMR spectroscopy does not provide detailed structural information about the CAP-Gly/MT interactions due to the large size of the complexes. On the contrary, the homonuclear DARR solid-state correlation spectra of CAP-Gly/MT assemblies indicate that magic angle spinning NMR spectroscopy can be used as a probe of their structure and dynamics, the knowledge of which is expected to contribute to our understanding of the mechanism of dynactin regulation of dynein-based cargo transport.

Acknowledgment. We are grateful to Kirk Czymmek and Deborah Powell at the Delaware Biotechnology Institute Bio-Imaging Center at the University of Delaware for their kind assistance with acquiring TEM images. The 21.1 T spectra were acquired at the Environmental Molecular Sciences Laboratory (EMSL), a national scientific user facility sponsored by the United States Department of Energy's Office of Biological and Environmental Research and located at Pacific Northwest National Laboratory in Richland, WA. Andrew Lipton, Jesse Sears, Michael Froehlke, Sarah Burton, David Hoyt, and Joseph Ford are thanked for their kind assistance during our visit to EMSL.

Supporting Information Available: Complete refs 19, 20, and 25, solution NMR spectra (HSQC and 3D heteronuclear correlation) illustrating resonance assignments of CAP-Gly in solution, comparison of torsion angles derived from solution and solid-state chemical shifts using TALOS with the torsion angles for other CAP-Gly structures, 14.1 T DARR spectra of free CAP-Gly acquired at different temperatures, dipolar-based DARR and J-based CTUC−COSY spectra of free CAP-Gly at 14.1 T, pulse sequences for resonance assignments by solid-state MAS NMR spectroscopy, HSQC spectra of CAP-Gly in the free form and in the presence of unpolymerized tubulin and weighted chemical shift changes versus residue number in CAP-Gly upon binding to the microtubules, solution chemical shifts of free CAP-Gly at pH 6.0 and 7.0, solid-state chemical shifts of free CAP-Gly prepared by controlled precipitation from PEG, chemical shift differences of free CAP-Gly in the solid state vs solution, acquisition and processing parameters for solid-state and solution NMR experiments, CD spectra of CAP-Gly, and sedimentation equilibrium experiments in CAP-Gly. This material is available free of charge via the Internet at http://pubs.acs.org.

JA902003U

(82) Stern, A. S.; Li, K. B.; Hoch, J. C. *J. Am. Chem. Soc.* **2002**, *124*, 1982–1993.
(83) Mobli, M.; Maciejewski, M. W.; Gryk, M. R.; Hoch, J. C. *J. Biomol. NMR* **2007**, *39*, 133–139.
(84) Laskowski, R. A.; Hutchinson, E. G.; Michie, A. D.; Wallace, A. C.; Jones, M. L.; Thornton, J. M. *Trends Biochem. Sci.* **1997**, *22*, 488–490.